

Tests of the Standard Model with Lepton Pair Production in e^+e^- Reactions

PLUTO Collaboration

Ch. Berger, A. Deuter, H. Genzel, W. Lackas, J. Pielorz^a, F. Raupach^b, W. Wagner^c

I. Physikalisches Institut der RWTH Aachen^d, D-5100 Aachen, Federal Republic of Germany

A. Klovning, E. Lillestøl

University of Bergen^e, N 5014 Bergen, Norway

J. Bürger, L. Criegee, F. Ferrarotto^f, G. Franke, M. Gaspero^f, Ch. Gerke^g, G. Knies, B. Lewendel,
J. Meyer, U. Michelsen, K.H. Pape, B. Stella^f, U. Timm, G.G. Winter, M. Zachara^h, W. Zimmermann
DESY, D-2000 Hamburg, Federal Republic of Germany

P.J. Bussey, S.L. Cartwrightⁱ, J.B. Dainton, B.T. King^j, C. Raine, J.M. Scarr, I.O. Skillicorn,
K.M. Smith, J.C. Thomson

University of Glasgow^k, Glasgow G12 8QQ, UK

O. Achterberg^l, V. Blobel, D. Burkart, K. Diehlmann, M. Feindt, H. Kapitza, B. Koppitz, M. Krügerⁿ,
M. Poppe, H. Spitzer, R. van Staa

II. Institut für Experimentalphysik der Universität Hamburg^d, D-2000 Hamburg, Federal Republic of Germany

C.Y. Chang, R.G. Glasser, R.G. Kellogg, S.J. Maxfieldⁿ, R.O. Polvado^o, B. Sechi-Zorn^a, J.A. Skard,
A. Skuja, A.J. Tylka, G.E. Welch, G.T. Zorn

University of Maryland^p, College Park, MD 20742, USA

F. Almeida^q, A. Bäcker, F. Barreiro, S. Brandt, K. Derikum^r, C. Grupen, H.J. Meyer, H. Müller,
B. Neumann, M. Rost, K. Stupperich, G. Zech

Universität-Gesamthochschule Siegen^d, D-5900 Siegen, Federal Republic of Germany

G. Alexander, G. Bella, Y. Gnat, J. Grunhaus

Tel-Aviv University^s, Tel-Aviv, Israel

H. Junge, K. Kraski, C. Maxeiner, H. Maxeiner, H. Meyer, D. Schmidt

Universität-Gesamthochschule Wuppertal^d, D-5600 Wuppertal, Federal Republic of Germany

Received 20 December 1984

^a Deceased

^b Now at Université de Paris Sud, F-91405 Orsay, France

^c Now at University of California, Davis, CA USA

^d Supported by the BMFT, Federal Republic of Germany

^e Partially supported by Norwegian Council for Science and Humanities

^f Rome University, partially supported by I.N.F.N., Sezione di Roma, Italy

^g Now at CERN, CH-1211 Geneva 23, Switzerland

^h Institute of Nuclear Physics, PL-30055 Cracow, Poland

ⁱ Now at Rutherford Appleton Laboratory, Chilton, UK

^j Now at University of Liverpool, UK

^k Supported by the U.K. Science and Engineering Research Council

^l Now at Texaco, D-2000 Hamburg, FRG

^m Now at Universität Karlsruhe, D-7500 Karlsruhe, FRG

ⁿ Now at University of Massachusetts, Amherst, Mass., USA

^o Now at Northeastern University, Boston, Mass., USA

^p Partially supported by the Department of Energy, USA

^q On leave of absence from Inst. de Fisica, Universidad Federal do Rio de Janeiro, Brasil

^r Now at BESSY, D-1000 Berlin, Germany

^s Partially supported by the Israeli Academy of Sciences and Humanities – Basic Research Foundation

Abstract. The differential cross section of the reaction $e^+ e^- \rightarrow e^+ e^-$ at a c.m. energy of 34.7 GeV has been measured. The result, together with our previously measured $e^+ e^- \rightarrow \mu^+ \mu^-$ data, are compared with the standard model predictions. We obtain for the weak neutral current couplings the values $g_v^2 = 0.09 \times 0.06$, $g_a^2 = 0.38 \times 0.08$. A fit of the Weinberg mixing angle gives the value $\sin^2 \vartheta_W = 0.13_{-0.02}^{+0.03} (1\sigma)_{-0.03}^{+0.08} (2\sigma)$. The data are also used to set limits on possible deviations from the pointlike structure of leptons. An upper limit for the $e^+ e^-$ coupling to a heavy spin 0 boson is also given.

Introduction

Electron positron processes at high energies can be used to test the Glashow-Salam-Weinberg (GSW) standard model of electroweak interactions [1, 2]. One of the best known examples is the observation of the μ -pair forward-backward asymmetry [3–12]. The weak contributions to Bhabha scattering and to μ -pair production [13] are described by diagrams similar to those of QED, where the virtual photon is replaced by the intermediate neutral vector boson, the Z_0 . These contributions allow the weak neutral current couplings, g_v^2 and g_a^2 , to be measured and resolve the ambiguity between the vector and the axial vector dominant solutions in the ν - e data [14].

The value of g_a can be measured from the μ -pair asymmetry which depends mainly on this axial coupling constant. Information on the vector coupling constant, g_v , can be obtained in two ways. The first is the determination of the total μ -pair cross section; however at the presently available $e^+ e^-$ energies this is only weakly dependent on g_v and thus requires a precise measurement. The second method is the study of Bhabha scattering, but again electroweak effects are expected to be small ($<4\%$). To obtain the most restrictive values for the electroweak parameters and in particular a value for $\sin^2 \vartheta_W$, both Bhabha scattering and μ -pair data have to be used simultaneously.

In as much as the data deviate from the standard model expectation they can be used to search for existence of composite or heavy leptons and photons. In general, any deviation can be represented by time-like, F_T , or space-like, F_S , form factors parametrized as follows [15],

$$F_T = 1 \pm \frac{s}{A_{T\pm}^2} \quad F_S = 1 \pm \frac{t}{A_{S\pm}^2} \quad (1)$$

where s and t are the usual Mandelstam variables and $A_{T\pm}$ ($A_{S\pm}$) are the QED time-(space-) like cut-off parameters to be determined by the experiment.

More specifically, a deviation from the standard model could be explained in terms of composite leptons as discussed in [16]. In this approach the contribution to the cross section as determined from an effective Lagrangian can be checked experimentally.

Recently, the possible existence of a spin 0 boson [17], X , has been discussed in connection with the apparent observation of Z_0 radiative decays [18]. This X boson, which is predicted by various composite models, is expected to couple to lepton pairs and thus should influence the lepton pair production in $e^+ e^-$ reactions in addition to the electroweak effects. Since the mass of this boson, if indeed it exists, is probably larger than our c.m. energy, its effect on the μ -pair production is small. Due to the interference between the space-like and time-like diagrams the influence of a spin 0 boson is enhanced in Bhabha scattering.

In this paper we describe the results obtained from our analysis [4] of the reaction $e^+ e^- \rightarrow e^+ e^-$ at a c.m. energy of 34.7 GeV. These data, in conjunction with our previously published μ -pair results at the same energy [3] and a subsequent improved analysis [4], are used to estimate the electroweak parameters and to search for deviations from the standard model [5].

Experimental Analysis

The data were taken with the PLUTO detector at the PETRA storage ring with an $e^+ e^-$ c.m. energy of 34.7 GeV. The PLUTO detector has been described elsewhere [19]. For the large angle Bhabha scattering events, only the barrel and end cap shower counters in conjunction with the inner track detector have been used. The track detector consisted of 13 cylindrical proportional chambers, each having copper coated cathode surfaces for reading the axial (z) coordinates. These chambers, together with the beam pipe, had a total thickness of 0.29 radiation lengths, so that showering of the scattered electrons had to be taken into account in the analysis.

The integrated luminosity was determined from small angle Bhabha events at polar angles ϑ between 6.8° and 13.6° using the forward spectrometer for track recognition and the respective shower counters for electron (e^\pm) identification. In this forward scattering region the contributions other than QED to the luminosity measurement are expected to be neg-

ligible. The forward track information enabled us to reduce systematic uncertainties due to measurement errors in the polar angle. The present analysis is based on a total integrated luminosity of $41.8 \times 1.0 \text{ pb}^{-1}$, where the error is mainly due to systematic uncertainties [4].

The large angle Bhabha events were selected using mainly the shower counter information according to the following criteria:

1. Two or three energy clusters were required in the shower counters, each one having an energy above one third of the beam energy.

2. At least one such cluster had to be associated with a track, which was then assigned to be an outgoing electron track. In fact, most of the events had two clusters associated with tracks. In those few cases (0.02% of the final sample) where all three clusters were associated with tracks, the two most energetic ones were taken to be electrons.

3. Events for which the fit for one of the tracks failed due to showering (2.3% of the final sample) were still accepted if they showed hits in the three innermost track chambers which were associated with a large cluster. The unobserved electron track direction was then derived from the shower cluster. The requirement of inner chamber hits was imposed to suppress $e^+ e^- \rightarrow \gamma\gamma$ events in which one photon had converted.

4. A remaining small fraction of multi-hadronic events was reduced by rejecting events with more than 5 tracks reconstructed to a common vertex in space, allowing at the same time for some electromagnetic shower tracks due to Bhabha scattering.

5. The acollinearity angle between the two electron tracks was required to be less than 15° .

6. The polar angle ϑ , averaged over the two electron tracks was restricted to $|\cos \vartheta| < 0.8$.

To determine the differential cross section from the final sample of 59,238 events, the following effects had to be accounted for:

1. Incorrect charge assignment which we estimated from the sample of events with two tracks of equal sign. The probability for charge misassignment for one track was found to be $\approx 5\%$ for $|\cos \vartheta| < 0.7$ and to increase very rapidly to 20% as $|\cos \vartheta|$ approaches 0.8. The uncertainty in this effect is included in the statistical errors and is found to be only significant at $\cos \vartheta \approx -0.8$.

2. Residual background from the processes $e^+ e^- \rightarrow \tau\tau$ (0.47%), $e^+ e^- \rightarrow \gamma\gamma$ (0.33%), $e^+ e^- \rightarrow \text{hadrons}$ (0.05%), and $\gamma\gamma \rightarrow e^+ e^-$ (0.05%).

3. Event losses due to data reduction (0.24%), data selection (0.53%), tracking failures (0.01%) and a small inefficiency in shower recognition in a limited region of the endcaps (0.56%).

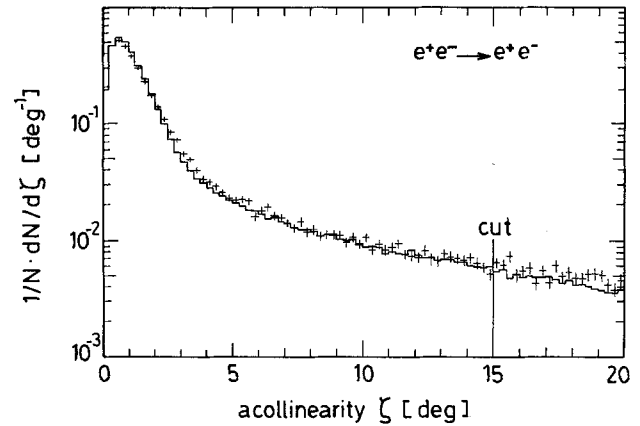


Fig. 1. Acollinearity distribution for the Bhabha scattering events (points) compared with generated data (histogram)

4. Radiative corrections related to the selection criteria 1, 5 and 6. These were calculated by using the electroweak Monte Carlo generator of Berends and Kleiss [20] which considers QED corrections up to the third order. In this Monte Carlo simulation the track directions and the energy deposited in the shower counters were randomly distributed around the generated values to simulate the measurement errors. The radiative corrections were then calculated from the ratio of the $\cos \vartheta$ distribution of the Monte Carlo events and the lowest order electroweak distribution. These corrections were found to be less than 4%.

We have checked the Monte Carlo simulation against the observed distributions and found them to agree with the data [4]. In Fig. 1 this comparison is shown for the acollinearity angle distribution. We estimate that the uncertainty in the overall detection efficiency due to the limited cluster energy resolution is below 0.8%. Here it should be noted that the contribution of higher order QED diagrams has not so far been calculated but is estimated to be less than 0.5% [21]. We have accounted for this contribution in the systematic error. An additional uncertainty of 0.5% arises from the hadronic vacuum polarization contribution [21]. Adding all these uncertainties in quadrature yields an overall systematic error of 0.5% to 2% depending on the value of $\cos \vartheta$. The contributions of the third order electroweak diagrams apart from pure QED were neglected in the Monte Carlo program. These contributions were recently calculated analytically [22] for an equivalent acollinearity angle cut (between 6° and 7°) which is harder than used here (15°). These calculated effects, when applied to our data, are found to be negligible in comparison with the statistical errors. Furthermore these third order contributions

Table 1. The differential cross section for Bhabha scattering. The quoted errors include also systematics apart from an overall normalization uncertainty of 2.6%

$\langle \cos \vartheta \rangle$	$s \cdot d\sigma/d\Omega$ [GeV ² · nb/str.]	$(\frac{d\sigma}{d\Omega})_{\text{exp}} / (\frac{d\sigma}{d\Omega})_{\text{QED}}$	$(\frac{d\sigma}{d\Omega})_{\text{exp}} / (\frac{d\sigma}{d\Omega})_{\text{GSW}}$
-0.750	24.0 ± 3.1	1.116 ± 0.143	1.120 ± 0.143
-0.650	22.8 ± 1.2	1.019 ± 0.054	1.031 ± 0.055
-0.550	22.9 ± 1.2	0.972 ± 0.050	0.990 ± 0.051
-0.450	23.2 ± 1.2	0.918 ± 0.047	0.939 ± 0.048
-0.350	30.4 ± 1.4	1.096 ± 0.050	1.125 ± 0.051
-0.250	30.3 ± 1.3	0.971 ± 0.043	0.998 ± 0.044
-0.150	34.8 ± 1.5	0.969 ± 0.041	0.996 ± 0.042
-0.050	42.0 ± 1.6	0.989 ± 0.038	1.014 ± 0.039
0.050	51.6 ± 1.8	0.994 ± 0.035	1.015 ± 0.036
0.150	67.4 ± 2.1	1.024 ± 0.031	1.040 ± 0.032
0.250	87.9 ± 2.3	1.011 ± 0.027	1.023 ± 0.027
0.350	122.8 ± 2.8	1.018 ± 0.023	1.024 ± 0.023
0.450	177.7 ± 3.5	1.000 ± 0.019	1.002 ± 0.020
0.525	253.5 ± 5.6	1.025 ± 0.023	1.024 ± 0.023
0.575	337.3 ± 6.7	1.055 ± 0.021	1.052 ± 0.021
0.625	431.6 ± 7.7	1.013 ± 0.018	1.010 ± 0.018
0.675	599.3 ± 9.5	1.015 ± 0.016	1.011 ± 0.016
0.725	889.0 ± 13.0	1.033 ± 0.015	1.029 ± 0.014
0.775	1,384.0 ± 18.0	1.028 ± 0.013	1.023 ± 0.013

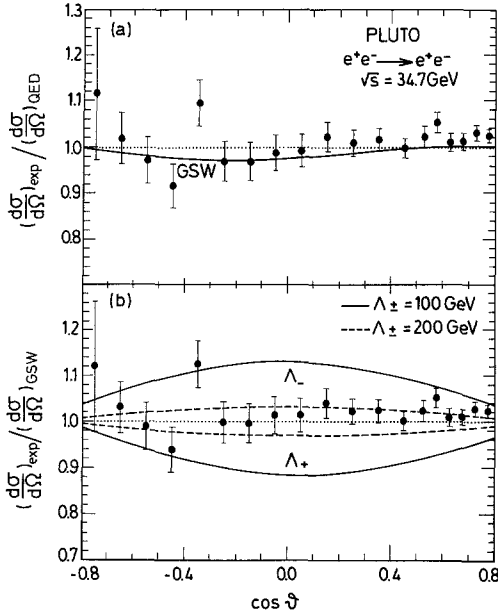


Fig. 2a and b. Differential cross section for Bhabha scattering normalized to **a** lowest order QED expectation; **b** standard model prediction with $m_Z=93 \text{ GeV}$, and $\sin^2 \vartheta_W=0.217$. The curve in **a** shows the standard model prediction. The curves in **b** are the expected distributions for several values of the QED cut-off parameters setting $A_{S\pm}=A_{T\pm}$. The curves above (below) the value 1.0 represent values for $\Lambda_{-}(\Lambda_{+})$

are expected to be even smaller for our softer acollinearity cut.

The resulting differential cross section, $s \cdot d\sigma/d\Omega$, for Bhabha scattering is given in Table 1. In the

same table we also present the differential cross sections normalized to the QED expectation and to the GSW model for a Z_0 mass of $m_Z=93 \text{ GeV}$ and $\sin^2 \vartheta_W=0.217$. These ratios are also shown in Fig. 2. The quoted errors are the statistical and systematic uncertainties added in quadrature. Not included is an overall normalization uncertainty due to the 2.6% error in the luminosity measurement.

Comparison with Models

General

Assuming $e-\mu$ universality, the cross section for Bhabha scattering and μ -pair production can be written in terms of the three Mandelstam variables s, t, u in the following general form,

$$\frac{d\sigma}{d\Omega} = \frac{\alpha^2}{2s} \left\{ \beta |A_1|^2 \left(\frac{s}{t}\right)^2 + |A_2|^2 \left(\frac{t}{s}\right)^2 + \frac{1}{2} (|A_3|^2 + |A_4|^2) \left(\frac{u}{s}\right)^2 + |A_5|^2 \right\}. \quad (2)$$

The parameter β is equal to 1 for Bhabha scattering and 0 for μ -pair production. For the standard model, the expressions for A_1 to A_5 are given in the first column of Table 2. The table also contains expressions for three proposed additional contributions to the amplitudes. Column 2 is the contribution of the time-like and space-like form factors given in (1), column 3 is the contribution of the composite model effective Lagrangian described below, and in column 4 the contribution of a spin 0 boson is listed.

The different models were studied by fitting their parameters to the data. To account for the luminosity uncertainty we have allowed its value, \mathcal{L} , to vary slightly around its measured value, \mathcal{L}_0 . Therefore we have added the term $(\mathcal{L} - \mathcal{L}_0)^2 / \Delta \mathcal{L}^2$ to the χ^2 function, where $\Delta \mathcal{L}$ is the uncertainty in \mathcal{L} . In those cases where the muon data have been included in the fit, the systematic uncertainty $\Delta \mathcal{K}$ in the ratio \mathcal{K} between the total numbers of μ -pair and Bhabha events had also to be taken into account. This was done by including an additional term $(\mathcal{K} - \mathcal{K}_0)^2 / \Delta \mathcal{K}^2$ in the χ^2 function, where \mathcal{K}_0 is the measured value. In all the fits \mathcal{L} and \mathcal{K} were found to be consistent with the measured values within their uncertainties.

The Standard Model (GSW)

The contribution of the weak neutral currents to the Bhabha and μ -pair cross sections can be most generally described using the 5 parameters: $g_v^2, g_a^2, \sin^2 \vartheta_W, m_Z$ and ρ . In the framework of electroweak theories, the coupling constants of charged leptons

Table 2. Expressions for the standard theory amplitudes A_1 to A_5 used in (2). The ΔA_1 to ΔA_5 are additional terms suggested by three different hypotheses. All symbols are explained in the text

	Standard model [13]		Form factor [15]	Composite models [16]	Spin 0 bosons [28]	
	QED	+ Weak				
A_1	1	$+(g_v^2 - g_a^2)\chi(t)$	ΔA_1	t/Λ_s^2	$\eta_{RL}t/\alpha\Lambda_c^2$	$\varepsilon\Gamma_{ee}t\xi(s)/\alpha sm_x$
A_2	1	$+(g_v^2 - g_a^2)\chi(s)$	ΔA_2	s/Λ_T^2	$\eta_{RL}s/\alpha\Lambda_c^2$	$\beta\varepsilon\Gamma_{ee}s\xi(t)/\alpha tm_x$
A_3	$1 + \beta s/t$	$+(g_v - g_a)[\chi(s) + \beta\chi(t)s/t]$	ΔA_3	$s/\Lambda_T^2 + \beta s/\Lambda_S^2$	$(1 + \beta)\eta_{RR}s/\alpha\Lambda_c^2$	0
A_4	$1 + \beta s/t$	$+(g_v + g_a)[\chi(s) + \beta\chi(t)s/t]$	ΔA_4	$s/\Lambda_T^2 + \beta s/\Lambda_S^2$	$(1 + \beta)\eta_{LL}s/\alpha\Lambda_c^2$	0
A_5	0	+0	ΔA_5	0	0	$[\beta(2 - \varepsilon)\Gamma_{ee} + (1 - \beta)]\sqrt{2\varepsilon\Gamma_{ee}\Gamma_{\mu\mu}} \cdot [\xi(s) + \beta\xi(t)]/\alpha m_x$

to the weak neutral current, g_v and g_a , are given by the following relation,

$$g_v^2 = (-\frac{1}{2} + 2 \sin^2 \vartheta_W)^2 + 4C \quad g_a^2 = 1/4. \quad (3)$$

In the GSW model C is equal to 0, but in non-gauge theories [23] and models with extended gauge groups [24], supersymmetry [25] or compositeness [26], C is larger than 0.

The parameter ρ is defined as $\rho \equiv m_W^2/(m_Z^2 \cos^2 \vartheta_W)$, where the mass of the W boson, m_W , is related to the Fermi coupling constant G_F , namely, $m_W^2 = \pi\alpha/[\sqrt{2}G_F \sin^2 \vartheta_W \cdot (1 - \Delta r)]$. Here $\Delta r = 0.0696$ is the radiative correction to m_W [27]. Thus ρ can be written in terms of m_Z and ϑ_W as,

$$\rho = \frac{\pi\alpha}{\sqrt{2}G_F m_Z^2 \sin^2 \vartheta_W \cos^2 \vartheta_W \cdot (1 - \Delta r)}. \quad (4)$$

The GSW model predicts ρ to be 1, whereas in less restrictive models, such as Ref. 1, ρ is a free parameter. The Bhabha and μ -pair cross section amplitudes are given in Table 2 in terms of g_a , g_v , and the function $\chi(s)$ given by

$$\chi(s) = \frac{\rho G_F}{2\sqrt{2}\pi\alpha} \cdot \frac{m_Z^2 s}{s - m_Z^2}. \quad (5)$$

In the fits to the data we chose to use as free parameters at most 2 out of the 5 electroweak variables mentioned above. The other parameters were substituted either by their standard model values or by taking the values measured in other types of experiments, or by using the relations (3) and (4).

In the first fit we used g_a^2 and g_v^2 as free parameters, setting ρ to the GSW prediction of 1, and m_Z to the averaged value of 93 GeV as measured in the $\bar{p}p$ collider by the UA1 and UA2 experiments [18]. In this case, as can be seen from (5), ϑ_W does not appear explicitly in the fit and in addition, at our energy, the dependence on m_Z is very weak. Using our Bhabha scattering data we obtain from the fit, $g_v^2 = 0.09 \times 0.12$ and $g_a^2 = 0.39 \times 0.20$. Next we include

in the fit also our μ -pair data [3, 4] which reduces the errors significantly, yielding the values

$$g_v^2 = 0.09 \times 0.06 \quad g_a^2 = 0.38 \times 0.08$$

with a $\chi^2/n_D = 22.5/25$. The values obtained for g_v^2 and g_a^2 are higher than the GSW expectation of 0.0044 (taking $\sin^2 \vartheta_W = 0.217$) and 0.25 but still within two standard deviations. These values are given in Table 3 together with previously reported measurements.

Figure 3 shows the 95% c.l. contour of the overall fit solution in the (g_a, g_v) plane. Also shown in the figure are the allowed regions (shaded areas) obtained from νe elastic scattering [14]. Almost complete overlap is seen between our result and the g_a -dominant solution of the νe experiments.

The vector coupling constant, g_v , is restricted by our g_v^2 result to the 95% c.l. interval of $-0.45 < g_v < 0.45$. From (3), assuming $C=0$, we then obtain the limits $0.02 < \sin^2 \vartheta_W < 0.48$ (95% c.l.). If we let C vary we obtain an upper limit for C of 0.050 (95% c.l.) by fixing $\sin^2 \vartheta_W$ to its currently used value of 0.217 [27]. We note that by setting ρ to 1, $\sin^2 \vartheta_W$ is determined only by the g_v value which is poorly evaluated from the differential cross sections. For that reason the Weinberg angle, ϑ_W , is only loosely constrained in this fitting method.

To measure $\sin^2 \vartheta_W$ directly it was chosen as a free parameter together with the Z mass. To this end we use (3) with $C=0$ and (5) where ρ was substituted from (4). The results are given in Fig. 4a where the 68% c.l. (solid line) and the 95% c.l. (dashed line) contours are shown in the $(m_Z, \sin^2 \vartheta_W)$ plane. The outer contour is compatible with the $\rho=1$ curve (dash-dotted line). The minimum χ^2 value of 22.5 with $n_D=25$ was obtained at the point $\sin^2 \vartheta_W = 0.13$ and $m_Z = 93$ GeV. Also shown in the figure is the combined $\bar{p}p$ measurement of m_Z and $\sin^2 \vartheta_W$. Taking the $\bar{p}p$ value of $m_Z = 93 \times 2$ GeV, we obtain

$$\sin^2 \vartheta_W = 0.13_{-0.02}^{+0.03}(1\sigma)_{-0.03}^{+0.08}(2\sigma).$$

Table 3. Summary of the electroweak parameters g_v^2 and g_a^2 , obtained from $e^+e^- \rightarrow l^+l^-$ reactions

Experiment	Data used	\sqrt{s} [GeV]	g_v^2	g_a^2
PLUTO [4]	$\mu\mu$	34.7	0.07 ± 0.10^a	0.38 ± 0.08^a
	ee	34.7	0.09 ± 0.12	0.39 ± 0.20
	$ee, \mu\mu$	34.7	0.09 ± 0.06	0.38 ± 0.08
JADE [6]	$ee, \mu\mu$	34.4, 42.4	0.02 ± 0.07	0.29 ± 0.02
TASSO [7]	$ee, \mu\mu$	34.5	-0.034 ± 0.052	0.220 ± 0.054
MARK J [8]	$ee, \mu\mu$	34.6, 39.8	0.05 ± 0.04	0.33 ± 0.05
CELLO [9]	$ee, \mu\mu, \tau\tau$	34.2	-0.03 ± 0.08	0.31 ± 0.12
MAC [10]	$\mu\mu$	29	0.07 ± 0.11	0.24 ± 0.04
MARK II [11]	$ee, \mu\mu, \tau\tau$	29	$0.03 \pm 0.03 \pm 0.03$	$0.23 \pm 0.05 \pm 0.02$
HRS [12]	$\mu\mu$	29	$0.027 \pm 0.051 \pm 0.089$	$0.208 \pm 0.064 \pm 0.021$
GSW expectation			0.0044^d	0.25

^a These values from [4] are results of an improved analysis of the data given in [3]. The corresponding μ -pair asymmetry is $-14.0 \times 3.2 \times < 1\%$

^b present analysis

^c using $\mu\mu$ data only

^d assuming $\sin^2 \vartheta_W = 0.217$

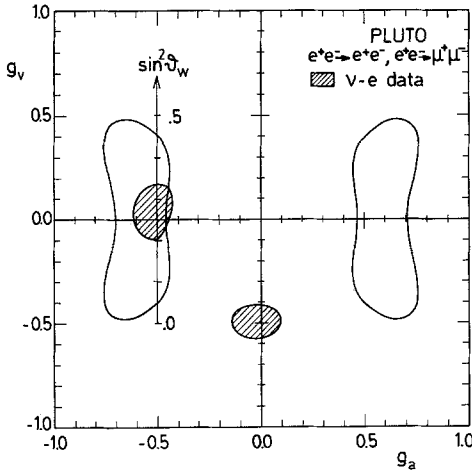


Fig. 3. Contours for 95% c.l. in the (g_v, g_a) plane obtained from the combined fit to the Bhabha scattering and μ -pair production data. The shaded area represents the allowed regions from v - e data [14]. The correspondence of g_v and $\sin^2 \vartheta_W$ is shown at the standard value of $g_a = -0.5$

This result is in good agreement with the MARK-J [8] value of 0.15 ± 0.04 and the JADE [6] result of 0.16×0.03 derived from μ -pair production using the same method. Our result is however lower than the values deduced from other than e^+e^- experiments [27] which are centred around 0.217×0.014 (after radiative corrections are applied) as also seen from the $\bar{p}p$ measurement which is close to our 95% c.l. contour. Nevertheless the value 0.217 is not ruled out by our data, since for that $\sin^2 \vartheta_W$ value we obtain a χ^2 of 26.9 for $n_D = 27$.

To explore the sensitivity of our data to the ρ parameter, a third fit was made where ρ and $\sin^2 \vartheta_W$

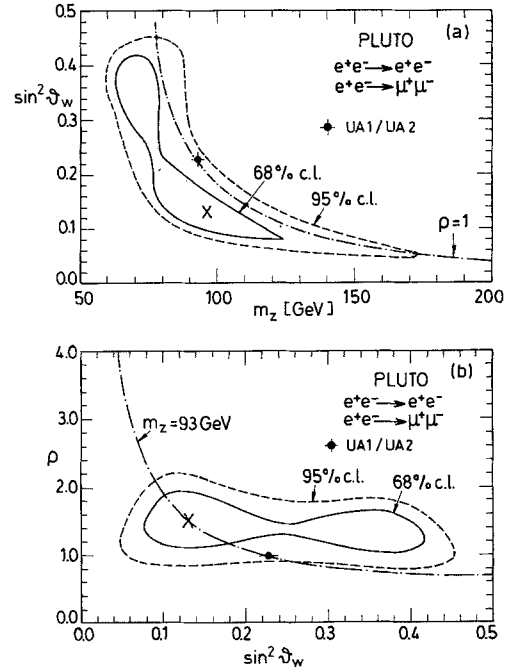


Fig. 4a and b. Contours for 68% and 95% c.l. obtained from a combined fit to our Bhabha and μ -pair data in the $(m_Z, \sin^2 \vartheta_W)$ plane **a** and $(\sin^2 \vartheta_W, \rho)$ plane **b**. The experimental point is the combined result from the $\bar{p}p$ collider taken from [18]. The dash-dotted lines represent the constraints $\rho=1$ in **a** and $m_Z=93$ GeV in **b**. The crosses in the figures represent the minimum χ^2 value

were the free parameters. In this fit m_Z was extracted from (4), and g_v^2 and g_a^2 were obtained from (3) setting $C=0$. The 68% (solid line) and 95% (dashed line) confidence level contours in the $(\sin^2 \vartheta_W, \rho)$ plane are shown in Fig. 4b, together with the average $\bar{p}p$ measurement. Our value of $\rho = 1.54 \times 0.28$ is

Table 4. Lower limits (95% c.l.) for the cut-off parameters $A_{S\pm}$ and $A_{T\pm}$ obtained from Bhabha scattering and μ -pair production

	$e^+e^- \rightarrow e^+e^-$		$e^+e^- \rightarrow \mu^+\mu^-$		Combined analysis	
	A_+ [GeV]	A_- [GeV]	A_+ [GeV]	A_- [GeV]	A_+ [GeV]	A_- [GeV]
A_S	184	162	–	–	204	174
A_T	143	104	206	141	349	146
$A_S=A_T$	184	162	–	–	346	175

Table 5. Lower limits (95% c.l.) for the composite scale parameter A_C calculated under different assumptions. The sign in the index of A corresponds to the \pm sign in the definitions 1 to 4 (see text)

Coupling	$e^+e^- \rightarrow e^+e^-$		$e^+e^- \rightarrow \mu^+\mu^-$		Combined analysis	
	A_{C+} [TeV]	A_{C-} [TeV]	A_{C+} [TeV]	A_{C-} [TeV]	A_{C+} [TeV]	A_{C-} [TeV]
RR, LL	1.1	0.76	2.9	0.86	^a	0.94
VV	2.2	1.9	2.4	1.6	4.1	2.1
AA	2.0	1.6	4.5	1.5	4.3	1.7

^a The calculation of the 95% c.l. is not possible since the fitted value for $1/A_{C+}^2$ is 2 s.d. below 0. For the 99% c.l. lower limit we obtain 8.4 TeV

2 s.d. higher than the GSW expectation of 1.0 and the results from the $\bar{p}p$ collider and from ν -reactions [18, 27]. Fixing m_Z the allowed region in the $(\sin^2 \vartheta_W, \rho)$ plane is a curve, which for $m_Z=93$ GeV passes through the region allowed by our data (see Fig. 4b).

Cut-Off Parameters

Possible deviations from the standard model are given in Table 2 in terms of the cut-off parameters $A_{S\pm}$ and $A_{T\pm}$. These contributions are added to the electroweak amplitudes and are then used to obtain lower limits on $A_{S\pm}$ and $A_{T\pm}$ from a fit to our data. In this fit, as well as the further fits discussed below, we have set the values of m_Z and $\sin^2 \vartheta_W$ to the world average values of 93 GeV and 0.217 respectively. Our lower limits for $A_{S\pm}$ and $A_{T\pm}$ are listed in Table 4. Similar cut-off limits were obtained by the other PETRA experiments [6–9]. In Fig. 2b the Bhabha cross section, normalized to the standard model prediction, is compared with predictions corresponding to different cut-off parameter values for $A_{S\pm}=A_{T\pm}$. We note that a cut-off parameter of 200 GeV verifies the validity of the standard model down to a distance of 10^{-18} cm.

Composite Scale Parameters

In [16] a general approach was proposed to describe composite models using the effective Lagrangian

$$L = (g^2/2A_C^2) \sum_{i,j=L,R} \eta_{ij} \cdot J_{i\lambda} \cdot J_j^2$$

where $J_{L,R}$ are the left-handed or right-handed leptonic currents. The parameter A_C , which sets the scale of the so-called “strong interaction” between the lepton constituents, is defined so that $g^2/4\pi=1$ and the coefficients η_{ij} are equal to 0 or ± 1 according to the particular assumption of the model listed below. The contributions of this effective Lagrangian to the amplitudes of the cross section formula (2) are listed in Table 2.

The following sets of values for the η_{ij} are usually considered [16]:

1. Left-handed currents, LL , where $\eta_{LL}=\pm 1$, $\eta_{RR}=\eta_{RL}=\eta_{LR}=0$.

2. Right-handed currents, RR , where $\eta_{RR}=\pm 1$, $\eta_{LL}=\eta_{RL}=\eta_{LR}=0$. This alternative cannot be distinguished from the former because they differ only by the negligible interference terms with the weak effect.

3. Vector currents, VV , where $\eta_{LL}=\eta_{RR}=\eta_{RL}=\eta_{LR}=\pm 1$. This choice has the same effect on the cross sections as the cut-off ansatz discussed in the preceding section, when $A_{S\pm}$ and $A_{T\pm}$ are replaced by $\sqrt{\alpha}A_C$.

4. Axial vector currents, AA , where $\eta_{LL}=\eta_{RR}=-\eta_{RL}=-\eta_{LR}=\times 1$.

The lower limits for the A_C parameters obtained from fits to our Bhabha and μ -pair data are listed in Table 5 for the different choices given above. Similar results were obtained by MAC [10], TASSO [7], and HRS [12] collaborations.

Spin 0 Bosons

Finally we discuss the effect of possible spin 0 bosons, X , with a mass, m_X , above our c.m. energy. Here we consider two X bosons, one being scalar and the other pseudoscalar with two hypotheses for the boson masses:

1. The mass of one of the two bosons is much higher than the other and its contribution can be neglected.

2. The masses of both bosons are equal.

The contributions of these bosons to the Bhabha and μ -pair cross section amplitudes [28] are listed in Table 2, where ε can be 1 or 2, depending on the number of spin 0 bosons contributing to the cross section according to the two hypotheses above. In the same table the function ξ is defined as $\xi(s)\equiv s/(s$

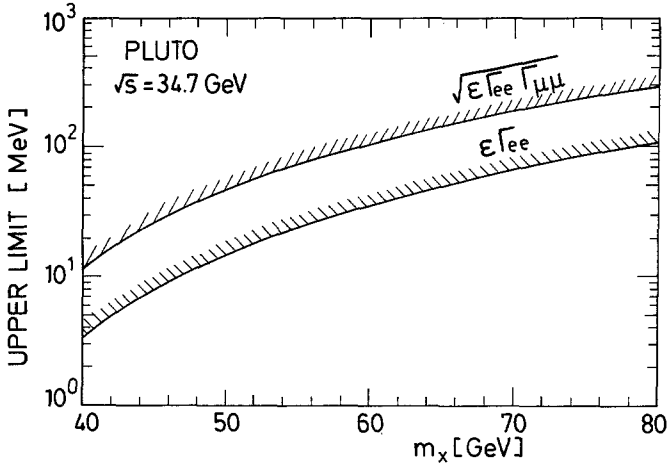


Fig. 5. Upper limits at the 95% c.l. of $\varepsilon\Gamma_{ee}$ and $\sqrt{\varepsilon\Gamma_{ee}\Gamma_{\mu\mu}}$ for a spin 0 boson decay into lepton pairs given as a function of its mass, m_X

$-m_X^2$) and Γ_{ee} ($\Gamma_{\mu\mu}$) are the $X \rightarrow e^+ e^-$ ($\mu^+ \mu^-$) partial widths. From fits to our data we obtain 95% c.l. upper limits on $\varepsilon\Gamma_{ee}$ and $\sqrt{\varepsilon\Gamma_{ee}\Gamma_{\mu\mu}}$, which are plotted in Fig. 5 as functions of m_X . Taking for example $m_X = 50$ GeV, we obtain $\varepsilon\Gamma_{ee} < 15$ MeV (95% c.l.). Similar limits have been obtained by other experiments [29].

Conclusions

The differential cross section for Bhabha scattering has been measured and used, together with our previously obtained μ -pair results, to test the standard model of electroweak interactions. This model can be expressed by alternative sets of variables. We have analysed our data in terms of the following pairs of parameters: (g_a^2, g_v^2) , $(m_Z, \sin^2 \vartheta_W)$, $(\sin^2 \vartheta_W, \rho)$, where in each case the other quantities in the model were taken from other measurements or extracted from the relations given by the model. From our fit, the best values obtained are $g_v^2 = 0.09 \times 0.06$ and $g_a^2 = 0.38 \times 0.08$, when ρ and m_Z are set to 1 and 93 GeV respectively. These values exceed by about 1.5 s.d. those expected in the GSW model with the currently accepted $\sin^2 \vartheta_W$ value of 0.217 ($g_v^2 = 0.0044$, $g_a^2 = 0.25$). When $\sin^2 \vartheta_W$ and m_Z are taken as the free parameters, they are found to be highly correlated. When m_Z is fixed at its directly measured value of 93 GeV, we obtain $\sin^2 \vartheta_W = 0.13_{-0.02}^{+0.03}$ (1σ) $_{-0.03}^{+0.08}$ (2σ). This value is consistent with previously measured values in μ -pair production and is 2.1 s.d. lower than the values obtained from the W and Z mass measurements and from ν -reactions. The third fit with $\sin^2 \vartheta_W$ and ρ as free parameters shows the relative insensitivity of $e^+ e^- \rightarrow l^+ l^-$ reactions to

the ρ value which varies within 95% c.l. between the values 0.99 and 2.08. The minimum χ^2 value is obtained at $\rho = 1.54$.

We have also used our data to investigate whether there is a need for modifications of the standard model. The lower limits of the cut-off parameters are found to be larger than 100 GeV (95% c.l.). For the composite scale parameters we obtain lower limits in the range of 1 TeV and above, at 95% c.l. Finally, no evidence is seen for the production of a heavy spin 0 boson. Assuming its mass to be 50 GeV, an upper limit of 15 MeV can be set for its partial width decay into $e^+ e^-$.

Acknowledgements. We are grateful to W. Hollik for a clarifying discussion. We wish to thank the members of the DESY directorate for the hospitality extended to the university groups. We are indebted to the PETRA machine group and the DESY computer centre for their excellent performance during the experiment. We gratefully acknowledge the efforts of all the engineers and technicians who have participated in the construction and maintenance of the apparatus.

References

1. S.L. Glashow: Nucl. Phys. **22**, 579 (1961)
2. S. Weinberg: Phys. Rev. Lett. **19**, 1264 (1967); A. Salam: Proc. 8th Nobel Symp., ed. N. Svartholm, p. 367. Stockholm: Almqvist and Wiksell 1968
3. PLUTO Collab. Ch. Berger et al.: Z. Phys. C - Particles and Fields **21**, 53 (1983)
4. H. Kapitzka: Ph.D. Thesis, Hamburg University, 1984
5. For our analysis of lepton pair production at lower energies see: PLUTO Collab. Ch. Berger et al.: Z. Phys. C - Particles and Fields **4**, 269 (1980); Z. Phys. C - Particles and Fields **7**, 289 (1981); Phys. Lett. **99B**, 489 (1981)
6. JADE Collab. W. Bartel et al.: Phys. Lett. **108B**, 140 (1982); Z. Phys. C - Particles and Fields **19**, 197 (1983); A.H. Ball: Proc. of the Int. Europhys. Conf. on High Energy Physics, Brighton (1983) p. 227; W. Bartel et al.: DESY Report 84-078
7. TASSO Collab. R. Brandelik et al.: Phys. Lett. **110B**, 173 (1982); Phys. Lett. **117B**, 365 (1982); M. Althoff et al.: Z. Phys. C - Particles and Fields **22**, 13 (1984)
8. MARK J Collab. D.P. Barber et al.: Phys. Lett. **95B**, 149 (1980); B. Adeva et al.: Phys. Rev. Lett. **48**, 1701 (1982); B. Adeva et al.: Phys. Rep. **109**, 133 (1984); L.G. Herten: Ph.D. Thesis, Aachen, 1983, AC Internal Report 83-05
9. CELLO Collab. H.-J. Behrend et al.: Phys. Lett. **103B**, 148 (1981); Z. Phys. C - Particles and Fields **14**, 283 (1982); Z. Phys. C - Particles and Fields **16**, 301 (1983)
10. MAC Collab. E. Fernandez et al.: Phys. Rev. Lett. **50**, 1238 (1983); SLAC-PUB-3133 (1983)
11. MARK II Collab. M.E. Levi et al.: Phys. Rev. Lett. **51**, 1941 (1983)
12. HRS Collab. D. Bender et al.: ANL-HEP-PR-84-03; M. Derrick et al.: ANL-HEP-PR-84-71
13. R. Budny: Phys. Lett. **55B**, 227 (1975)
14. W. Krenz: University of Aachen Preprint, PITHA 82/26 (1982)
15. S.D. Drell: Ann. Phys. **4**, 75 (1958)
16. E.J. Eichten et al.: Phys. Rev. Lett. **50**, 811 (1983); M. Abolins et al.: Proc. of the Division of Particles and Fields Summer Study on Elementary Particle Physics and Future Facilities, Snowmass, Colorado, p. 274 (1982)

17. U. Baur et al.: Phys. Lett. **135 B**, 313 (1984); R.D. Peccei: Phys. Lett. **136 B**, 121 (1984); H. Fritzsch, H. Faissner: MPI-PAE/PTh 76/83, Munich (1983); F.M. Renard: Phys. Lett. **139 B**, 449 (1984)
18. UA1 Collab. G. Arnison et al.: Phys. Lett. **122 B**, 103 (1983); Phys. Lett. **126 B**, 398 (1983); Phys. Lett. **129 B**, 273 (1983); Phys. Lett. **134 B**, 469 (1984); Phys. Lett. **147 B**, 241 (1984); UA2 Collab. M. Banner et al.: Phys. Lett. **122 B**, 476 (1983); P. Bagnaia et al.: Phys. Lett. **129 B**, 130 (1983)
19. L. Criegee, G. Knies: Phys. Rep. **83**, 153 (1982); PLUTO Collab. Ch. Berger et al.: Z. Phys. C – Particles and Fields **26**, (1984)
20. F.A. Berends, R. Kleiss: Nucl. Phys. **B 228**, 537 (1983)
21. H. Burkhardt: Ph.D. Thesis, Hamburg University, 1982, DESY Internal Report F35-82-03
22. M. Böhm et al.: Phys. Lett. **144 B**, 414 (1984); A. Denner: Diplomarbeit, Würzburg University, 1984
23. P.Q. Hung, J.J. Sakurai: Nucl. Phys. **B 143**, 81 (1978); J.D. Bjorken: Phys. Rev. **D 19**, 335 (1979)
24. E.H. de Groot et al.: Phys. Lett. **90 B**, 427 (1980); Phys. Lett. **95 B**, 128 (1980); V. Barger et al.: Phys. Rev. Lett. **44**, 1169 (1980); Phys. Rev. **D 22**, 727 (1980)
25. P. Fayet: Proc. XXI Int. Conf. on High Energy Physics, Paris, 1982 on J. Phys. (Paris) Suppl. **43**, C3-673 (1982)
26. R. Kögerler: Electroweak Interactions at High Energies, Proc. of the 1982 DESY Workshop, p.296, eds. R. Kögerler, D. Schildknecht. Singapore: World Scientific 1983
27. W.J. Marciano, A. Sirlin: Phys. Rev. **D 29**, 945 (1984)
28. F.W. Bopp et al.: SI-83-24 (1983) and SI-84-3 (1984), Siegen University, Z. Phys. C – Particles and Fields (in press); W. Hollik et al.: Phys. Lett. **140 B**, 424 (1984)
29. CELLO Collab. H.-J. Behrend et al.: Phys. Lett. **140 B**, 130 (1984); MARK J Collab. B. Adeva et al.: MIT LNS Technical Report no. 134 (1984)